

Generate Realistic Test Scenes for V2X Communication Systems

An Guo^{ib}, Xinyu Gao^{ib}, Chunrong Fang^{ib}, Haoxiang Tian^{ib}, Weisong Sun^{ib},
Yanzhou Mu^{ib}, Shuncheng Tang^{ib}, Lei Ma^{ib}, and Zhenyu Chen^{ib}

Abstract—Accurately perceiving complex driving environments is essential for ensuring the safe operation of autonomous vehicles. With the tremendous progress in deep learning and communication technologies, cooperative perception with Vehicle-to-Everything (V2X) technologies has emerged as a solution to overcome the limitations of single-agent perception systems in perceiving distant objects and occlusions. Despite the considerable advancements, V2X cooperative perception systems require thorough testing and continuous enhancement of system performance. Given that V2X driving scenes entail intricate communications with multiple vehicles across various geographic locations, creating V2X test scenes for these systems poses a significant challenge. Moreover, current testing methodologies rely on manual data collection and labeling, which are both time-consuming and costly.

In this paper, we design and implement V2XGEN, an automated testing generation tool for V2X cooperative perception systems. V2XGEN utilizes a high-fidelity approach to generate realistic cooperative object instances and strategically place them within the background data in crucial positions. Furthermore, V2XGEN adopts a fitness-guided V2X scene generation strategy for the transformed scene generation process and improves testing efficiency. We conduct experiments on V2XGEN using multiple cooperative perception systems with different fusion schemes to assess its performance on various tasks. The experimental results demonstrate that V2XGEN is capable of generating realistic test scenes and effectively detecting erroneous behaviors in different V2X-oriented driving conditions. Furthermore, the results validate that retraining systems under test with the generated scenes can enhance average detection precision while reducing occlusion and long-range perception errors.

Index Terms—Software testing, automated test generation, V2X cooperative driving



1 INTRODUCTION

Autonomous vehicles are increasingly becoming an integral part of daily life [1]. As a prime example of safety-critical intelligent software, autonomous driving systems (ADSs) depend on perception components to interpret information about the surrounding environment and relay perception results to downstream decision modules, thereby ensuring the smooth operation of the system. Recent advancements in deep learning and sensor technology have significantly enhanced the performance of modern perception systems [2], [3]. Despite these remarkable developments, single-agent perception systems often produce inaccurate or incomplete

results due to inherent single-view constraints, such as occlusion and sparse sensor observations at a distance. These limitations can lead to incorrect system behavior or even severe accidents [4], [5].

Vehicle-to-everything (V2X) technology has garnered significant attention in recent years due to its potential to overcome the limitations of single-agent perception in detecting occlusions and long-range obstacles [6]–[8]. V2X communication systems enable autonomous driving systems to leverage cooperative perception strategies to integrate additional perception information from diverse viewpoints provided by cooperative vehicles (CVs) and traffic infrastructure, thereby enhancing comprehensive environmental awareness. Numerous leading manufacturers and organizations, including Audi, Tesla, and Baidu, are actively developing V2X platforms to enable autonomous driving systems to accurately perceive their surroundings in challenging traffic scenes [9], [10].

To ensure continuous improvement of the V2X system, developers must build two typical types of V2X application scenes (i.e., occlusion and long-range perception in the ego vehicle’s viewpoint) to iteratively test and optimize V2X systems’ corresponding basic functionality [8], [11], [12]. However, in practice, building test scenes for V2X systems is a labour-intensive and time-consuming task. It requires practitioners to deploy specific V2X-related infrastructure during real-world road testing to collect data from various traffic scenes [13], [14]. In addition, they must manually annotate the data collected from cooperative vehicles (e.g.,

- An Guo, Xinyu Gao, Chunrong Fang, Yanzhou Mu, and Zhenyu Chen are with the State Key Laboratory for Novel Software Technology, Nanjing University, China. (E-mail: guoan218@smail.nju.edu.cn, xinyugao@smail.nju.edu.cn, fangchunrong@nju.edu.cn, 602022320006@smail.nju.edu.cn, zyichen@nju.edu.cn)
- Haoxiang Tian is with the Institute of Software, Chinese Academy of Sciences, China. (E-mail: tianhaoxiang20@otcaix.iscas.ac.cn)
- Weisong Sun is with the Nanyang Technological University, Singapore. (E-mail: weisong.sun@ntu.edu.sg)
- Shuncheng Tang is with the University of Science and Technology of China, Hefei, China. (E-mail: scott@mail.ustc.edu.cn)
- Lei Ma is with the University of Tokyo, Tokyo 113-8658, Japan, and also with the University of Alberta, Edmonton, AB T6G 1H9, Canada. (E-mail: ma.lei@acm.org)

Manuscript received xxx xxx, 2025; revised xxx xxx, 2025.

images, point clouds, etc.) and thoroughly examine the visualization results to ensure that the scenes are annotated correctly [11], [15]. Despite these efforts, the collected scenes struggle to support testing the V2X system adequately due to the large input space, which encompasses various sensor data from individual agents. Thus, there is an urgent need for a more efficient approach to building test scenes.

Software engineering researchers have proposed several testing techniques by generating testing scenes to assess the potential risks of perception systems in the real world [16]–[18]. However, these methods mainly focus on testing single-agent perception systems and are difficult to apply to V2X scenes. Due to their disregard for the involvement of cooperative vehicles, these methods face challenges in generating test scenes related to the basic V2X functionalities that are of interest to developers (e.g., the ego vehicle encounters occlusion challenges while the cooperative vehicle has an unobstructed view). Moreover, testing V2X systems requires that the generated test data for different agents be consistent with their perspectives (e.g. a vehicle should appear differently because of the varying viewing angles of traffic participants). Due to the inherent nature of V2X, which involves multi-vehicle collaboration in heterogeneous and complex environments, simply applying a single-agent test method to each agent individually cannot guarantee this consistency, resulting in unrealistic and implausible generated data.

To address these challenges, we propose V2XGEN, an automated testing method that generates realistic and V2X-interested scenes for V2X cooperative perception systems. V2XGEN incorporates five realistic transformation operators grounded in metamorphic testing theory, thereby minimizing the cost of manual data collection and labeling. Each operator is carefully designed, taking into account the operational mechanisms of V2X systems in the physical world, to ensure that the transformed scenes are semantically plausible. By flexibly utilizing and combining these operators, V2XGEN can manipulate entities within the original data or insert new entities to generate new realistic scenes. Moreover, V2XGEN employs a fitness-guided approach to guide entity manipulation, facilitating the generation of more V2X-interested and challenging test cases for the systems under test. Finally, V2XGEN leverages metamorphic relations between the synthesized data and the seed data to automatically identify erroneous perception results.

To evaluate the effectiveness and efficiency of V2XGEN, we conduct experiments on six popular cooperative perception systems with distinct information fusion schemes to assess the efficacy of V2XGEN. Qualitative and quantitative experiments demonstrate that V2XGEN can generate realistic test data that meet test input specifications for cooperative perception systems. Our subsequent experimental results reveal that V2XGEN, when using the fitness-guided V2X scene generation method, produces more failed tests on cooperative perception systems compared to CooTest [15] and V2XGEN_N (w/o fitness-guided strategy) baselines. We further retrain the selected cooperative perception systems with test data generated by V2XGEN, finding that the system performance (measured by average precision) can be improved.

The main contributions of this paper are summarized as

follows:

- **Method.** We propose an automated testing approach for V2X cooperative perception systems based on fitness-guided metamorphic testing. Specifically, we leverage several high-fidelity transformation operators to manipulate entities in the test seed to generate realistic scenes.
- **Tool.** We implement the above method into a tool V2XGEN. V2XGEN is an automated scene-generation tool for testing cooperative perception systems. We have released V2XGEN and the cooperative scenes generated by V2XGEN at <https://sites.google.com/view/v2xgen/>.
- **Evaluation.** We conduct extensive experiments to evaluate the performance of V2XGEN across six cooperative perception systems. The results demonstrate that V2XGEN can generate realistic test scenes and efficiently detect erroneous system behaviors. Furthermore, retraining the cooperative perception system using the generated test scenes significantly enhances its performance.

2 BACKGROUND

2.1 V2X Cooperative Perception System

Autonomous driving systems consist of sequentially operating subsystems. Figure 1 illustrates the architecture of an autonomous driving software system based on contemporary designs. The perception module is responsible for processing environmental information collected by various sensors to facilitate functionalities such as object detection and tracking. Upon receiving the processed perception data, the planning module estimates future trajectories for the detected obstacles. Finally, the control module calculates and executes the planned trajectory. As the foundation of autonomous driving, perception is essential for environmental understanding.

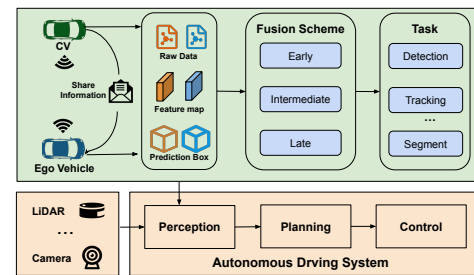


Fig. 1. The architecture of cooperative perception systems in autonomous driving.

However, the inherent limitations of camera and LiDAR devices, particularly regarding occlusions and long-distance perception, pose significant challenges for autonomous driving systems designed for individual vehicles [19]. These challenges can result in severe consequences in complex traffic scenes. In contrast, cooperative perception enhances multi-vehicle detection by leveraging V2X communication, enabling vehicles and infrastructure to share sensing data. This collaboration provides multiple perspectives on obstacles, compensating for individual limitations [20], [21]. The integrated data is subsequently utilized by the perception

system as input to generate more accurate environmental predictions.

V2X cooperative perception is classified into early fusion, late fusion, and intermediate fusion [11]. Early fusion shares raw data with nearby agents, allowing the ego vehicle to aggregate and predict objects [22]. Late fusion transmits detection outputs and integrates proposals [23]. Intermediate fusion balances bandwidth and accuracy by encoding raw data into vector representations before sharing [24], [25].

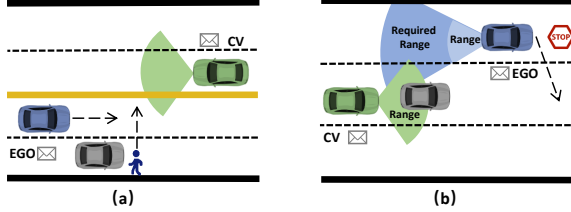


Fig. 2. Motivating examples illustrating the core functionalities of V2X cooperative perception systems.

Motivating Examples. The examples in Figure 2 highlight the importance of V2X collaborative perception. In Figure 2 (a), a green cooperative vehicle in the opposite lane helps the blue ego vehicle detect an occluded pedestrian. In Figure 2 (b), the blue ego vehicle prepares to change lanes. The gray vehicle, positioned farther from the ego vehicle, is within the blue ego vehicle's blind spot and requires assistance from the green cooperative vehicle to enhance its perception range.

2.2 The Preliminaries of Cooperative 3D Object Detection

Cooperative 3D object detection is a fundamental perception task for V2X communication systems, enabling ADS to fully comprehend external environments. In cooperative 3D object detection, the cooperative perception system CP takes a multi-view scene data s as input, which consists of an ego vehicle's point cloud P_{ego} and point clouds $P_{coo} = \{P_{cv_i}\}_{i=1}^n$ from the observation perspectives of n cooperative vehicles cv_i . The system then outputs a bounding box for each detected object based on the relative position of the ego vehicle, providing its 3d location $loc = [x, y, z]$, dimensions l (length), w (width), h (height), and orientation through a heading angle yaw . The accuracy of cooperative 3D object detection is typically measured by Intersection over Union (IoU) [26]. The IoU computation is defined as $IOU = \text{area}(B_p \cap B_{gt}) / \text{area}(B_p \cup B_{gt})$. This metric quantifies the overlap area between a ground-truth 3D bounding box in bird's-eye view, B_{gt} , and a predicted 3D bounding box in bird's-eye view, B_p , relative to their union [13]. An object is considered successfully detected if the IoU exceeds a specified threshold, γ . In this study, we set the IoU threshold, γ , to 0.5, in alignment with prior research [15].

3 APPROACH

In this section, we present the design and implementation of V2XGEN, a tool devised for automated test generation of

the V2X cooperative perception module within ADS. In Figure 3, the developer initiates the process by selecting seeds from real-world V2X scenes. Subsequently, V2XGEN then applies the metamorphic relations specifically defined for cooperative perception systems. It is equipped with two basic transformation operators (i.e., insertion and deletion) and three composite transformation operators (i.e., scale, translation, and rotation), which are combinations of the basic operators. The design of these transformation operators in V2XGEN considers the operational mechanism of the V2X cooperative perception system in the physical environment, allowing for flexible combinations to generate realistic, practical application scenes. Through the use of a fitness metric, V2XGEN efficiently selects test scenes likely to reveal functional potential errors such as occlusion and long-range perception errors in the systems. The transformed test scenes are then generated to assess the performance of the cooperative perception system in autonomous driving. Finally, V2XGEN generates test reports containing average precision (AP), occlusion perception errors, and long-range perception errors based on systems' predicted bounding boxes. Moreover, V2XGEN can enhance the system's cooperative perception performance through retraining with generated transformed scenes.

3.1 Definitions

To efficiently construct challenging test scenes involving occluded and long-range objects, as well as to evaluate the performance of the V2X cooperative perception system in two types of typical application scenes, we define two unique V2X cooperative object detection errors: *Occlusion Perception Error (OE)* and *Long-range Perception Error (LE)*. Specifically, occlusion perception error refers to the inability of the cooperative vehicle to assist the ego vehicle in identifying occluded objects. Given an object $o \in \mathbb{O}$ to be detected, a ground-truth bounding box $B_{gt} \in \mathbb{GT}$ and a predicted bounding box $B_p \in \mathbb{DT}$ of cooperative perception system, occlusion perception error can be formalized as:

$$\exists B_{gt} \in \mathbb{GT}, Occ_{ego}(o) > 0 \wedge \forall B_p \in \mathbb{DT}, 0 \leq IOU(B_{gt}, B_p) \leq \gamma \quad (1)$$

, where $Occ_{ego}(o)$ is the line-of-sight occlusion rate of the ego vehicle detecting object o . Occlusion perception error typically occurs when the object o intended for detection is occluded by other obstacles within the ego vehicle's field of view. Long-range perception error refers to the cooperative vehicle's inability to assist the ego vehicle in identifying objects at long distances, which can be formalized as:

$$\exists B_{gt} \in \mathbb{GT}, Dis^{ego}(o) > k \wedge \forall B_p \in \mathbb{DT}, 0 \leq IOU(B_{gt}, B_p) \leq \gamma \quad (2)$$

, where $Dis^{ego}(o)$ represents the distance between the ego vehicle and the detected object o , and k is the distance parameter for long distances in the cooperative perception dataset.

3.2 V2X Scene Transformation Operators

One significant threat to generate realistic test scenes for V2X systems is the requirement to synthesize perspective-consistent scenes for each agent in V2X systems. This means objects in each scene should appear differently depending on the viewpoint of the vehicle. For instance, as depicted in

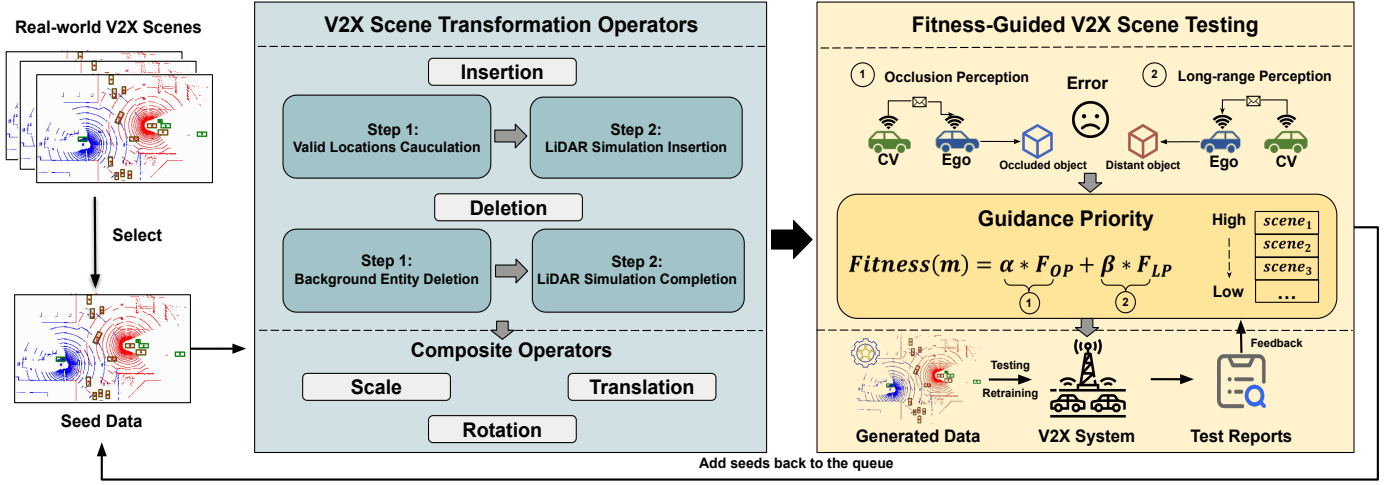


Fig. 3. The workflow of V2XGEN.

Figure 4 (b), from the ego vehicle’s perspective, the yellow car is partially obscured by the grey car, while the green cooperative vehicle has an unobstructed view. To address this, we establish perspective transformation between multi-agents and further design five transformation operators for V2X scenes, including two basic operators (entity insertion and deletion) and three composite operators (scale, rotation, and translation) built upon basic operators. Each operator manipulates entities based on multi-agent perspective transformation and real-world physics laws to generate perspective-consistent and realistic test scenes.

3.2.1 Multi-agent Perspective Transformation

The V2X communication system needs to determine the positional transformation matrix between multiple agents to ensure that the perception information measured in different local coordinate systems can be converted to each other. Therefore, we uniformly establish a world coordinate system to represent this transformation. The transformation from the world coordinates to the vehicle V_x ($x \in \{ego, cv_i\} | i \in 1, 2, \dots, n\}$) can be expressed as:

$$p_{V_x}^t = T_{world \rightarrow V_x}^t \cdot p_{world} \quad (3)$$

, where p_{world} is a location $[\omega_{x_0}, \omega_{y_0}, \omega_{z_0}, 1]^T$ of world coordinate system, $T_{world \rightarrow V_x}^t \in \mathbb{R}^{3 \times 4}$ is coordinate transformation matrix from world coordinate system to the local coordinate system of participant V_x at the time t , and $p_{V_x}^t$ is the location of the participating vehicle V_x in the cooperative perception system at the time t . Based on Equation 3, we can apply the transformation matrix to convert the world coordinates to that of any participating vehicle’s perspective. Conversely, the participating vehicle can use the corresponding inverse matrix to transform back to the world coordinate system. Based on this transformation mechanism, the operator we designed strictly ensures perspective consistency.

3.2.2 Insertion Operator

The insertion operator (IS) is designed to generate plausible new point cloud scenes s' by adding entities into the original multi-view scene $s = \{P_{ego}, P_{cv_i} | i \in 1, 2, \dots, n\}$. Given an entity instance e_{ins} selected from the entity assets \mathbb{E} ,

V2XGEN first calculates valid locations and orientations of the entity to be inserted for each view. Then V2XGEN leverages a set of virtual LiDARs to render the entity instance as object-level point clouds and integrate them into the scene at the corresponding viewpoints correctly by processing their interaction with background objects. We detail each step of the insertion operator below.

Step 1. Valid Locations Calculation. Inserting entities at appropriate locations is crucial for synthesizing realistic test scenes. The location of each inserted entity must be reasonable (e.g., a vehicle should be correctly placed on the road) and adhere to the requirement of the transformation relationship outlined in Section 3.2.1 across multiple views. To compute feasible candidate insertion points, V2XGEN first employs semantic segmentation model [27] to separate the road point cloud from the ego-perspective point cloud P_{ego} and each cooperative point cloud P_{cv_i} , respectively. Then, V2XGEN computes the insertion point in the world coordinate system and filters out points that are not on the road surface in any of the views based on Equation 3 to ensure that all candidate locations are valid from each viewpoint. Moreover, given an entity e_{ins} with specific orientation and dimensions, inserting the entity at a candidate location may result in a collision with the objects in the background scene s . To address this, V2XGEN calculates the 3D bounding box B_e for the entity instance to be inserted and checks if the 3D box B_e contains any other objects in the background scene for each view. If the IOU between B_e and all the background bounding boxes is 0, V2XGEN considers this selected location to be non-colliding. Besides, to guarantee that at least one cooperative vehicle can detect the inserted entity, V2XGEN computes occlusion rates of the entity from multiple views and ensures that the occlusion rate from at least one cooperative vehicle’s perspective remains below 90%.

Step2. LiDAR Simulation Insertion. Given a candidate location $loc = \{loc_{ego}, loc_{cv_i} | i \in 1, 2, \dots, n\}$ for insertion, this step aims to render the entity instances into original scene $s = \{P_{ego}, P_{cv_i} | i \in 1, 2, \dots, n\}$ respectively to generate new perspective-consistency scene s' . The realism of the synthesized scene depends on two key factors: ensuring the inserted entities maintain the perspective consistency across

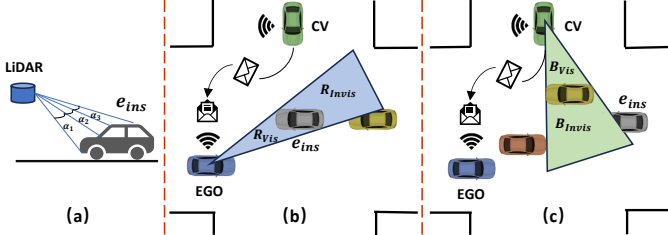


Fig. 4. Virtual LiDAR equipped by the V2X cooperative perception system emitting lasers to hit the inserted entity e_{ins} . (a) View along the y-axis, (b) and (c) top view.

multiple views, and ensuring these entities conform to the physics laws in each individual view. To address this, we leverage a high-fidelity approach to simulate the operational mechanism of cooperative perception LiDAR in the physical world. Specifically, we create a multi-view virtual LiDAR sensor set for the V2X scene generation. Each participant in the system is equipped with a configurable virtual LiDAR, initialized based on the real-world LiDAR configuration in the V2X system (e.g., the field of view, the number of beams, etc). The virtual LiDAR utilizes a ray-casting algorithm to simulate the real laser beam emission, thereby rendering the inserted entity e_{ins} as an object-level point cloud consistent with the viewpoint. Figure 4 (a) illustrates the ray-casting process of a nonlinear LiDAR in a V2X system. Moreover, we process interaction with background objects in the scene at each viewpoint. For each viewpoint, we delete the point clouds occluded by the inserted entity in the scene and remove the occluded parts in the inserted entity according to the geometric relationship. Figure 4 (b) and Figure 4 (c) show the processing in different views. In Figure 4 (b), the ray from the ego vehicle's virtual scanner intersects with the inserted entity e_{ins} , forming visible region R_{vis} and invisible region R_{invis} , where V2XGEN removes points in R_{invis} . In Figure 4 (c), the inserted entity e_{ins} is partially occluded by the yellow background object in the cooperative vehicle's view, V2XGEN then removes occluded parts in B_{invis} .

3.2.3 Deletion Operator

The deletion operator (DL) is designed to generate a realistic new scene by removing entities in multiple views and reconstructing the previously occluded areas. Our core idea is that deletion may alter the occlusion relationships among objects, thereby affecting the reasoning confidence of the cooperative perception system. Given the entity instances selected for deletion from the cooperative perception data recorded in the real world, V2XGEN first deletes the selected background entity by filtering the points within the object's ground truth box. Then, V2XGEN leverages the high-fidelity virtual LiDAR simulation to fill the occlusion area of the selected entity. We detail each step of the deletion operator below.

Step 1. Background Entity Deletion. V2XGEN first randomly selects an entity instance e_{del} for deletion from the cooperative perception scene and determines candidate location $loc = \{loc_{ego}, loc_{cv_i} | i \in 1, 2, \dots, n\}$ for viewpoint based on Equation 3. Then, for each participant's viewpoint, V2XGEN calculates the entity's 3D bounding box B_e based on ground truth and deletes all point clouds contained within B_e to remove the background entity.

Step 2. LiDAR Simulation Completion. After deleting entities' point clouds, V2XGEN leverages a high-fidelity occlusion-completion strategy based on virtual sensor simulation to reconstruct the previously occluded background ground and objects. We leverage the multi-view virtual LiDAR sensor set to infer the invisible occlusion region of the selected entity instance e_{del} and sequentially complement the ground and objects in the invisible area. To complete the ground, we meshify the road point cloud to reconstruct the road surface and leverage the ray casting algorithm to complete the obscured ground with realistic scan lines. In order to complete the background objects, we compute the intersection of the occluded region with the bounding boxes of all background objects to identify those that were occluded by the deleted entity e_{del} . We then reinsert entities of the same size as the originals at the locations of each occluded object and leverage the multi-view virtual LiDAR sensor set to reconstruct the occluded object under each view. Figure 5 presents the visualization of ego-vehicle data and aggregated LiDAR data before and after entity deletion. It is evident that our technology excels in entity deletion and LiDAR simulation completion, including occluded objects and ground completion.

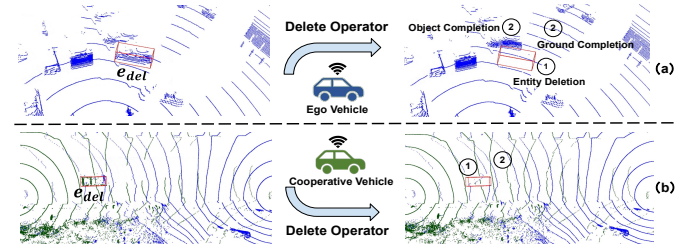


Fig. 5. Subfigures (a) and (b) illustrate the visualization effects of ego vehicle data and aggregated LiDAR data, respectively, generated by V2XGEN after the application of the deletion operator. The entities selected for deletion by V2XGEN are marked in red.

3.2.4 Composite Operators

In the scene of cooperative perception, the shapes of objects within a single class can vary significantly (e.g., flat sports cars and round vintage cars [28]). Such long-tail data have the potential to be misclassified. Additionally, dynamic changes in the heading directions and locations of objects can adversely affect the positioning accuracy of cooperative perception systems [29], [30]. Therefore, we utilize scale, rotation, and translation operators to simulate objects with various shapes, orientations, and positions in the real world. We regard these operators as a combination of insertion and deletion operators to ensure the realism of the generated scenes. The combined operators inherently conform to the laws of physics and maintain perspective consistency since each basic operator in the composition is rigorously designed to ensure these natures. We provide the details of each operator below.

Scale Operator. The scale operator (SC) changes the shape of the object. The operator first randomly selects the entity to be scaled from the multi-view cooperative perception scene s . For each participant's viewpoint, it deletes an entity with length x , width y , and height z and then inserts a new entity with a length $s_x * x$, width $s_y * y$, and height $s_z * z$ respectively, where s_x , s_y , and s_z are the scale ratios.

To ensure realism, this operator sets conservative scale parameters ($s_x \in [0.9, 1.1]$, $s_y \in [0.9, 1.1]$, $s_z \in [0.9, 1.1]$) and automatically calculates the position of the entity to ensure that it is placed on the ground.

Rotation Operator. The rotation operator (RO) changes the direction of the object. The operator first randomly selects the entity to be rotated from the multi-view cooperative perception scene s . For each participant's viewpoint, it deletes the entity with the original orientation of r_z and inserts the entity with the orientation of $r_z + rot$. rot is the rotation angle around the upright z axis. To ensure realism, the operator sets conservative rotation parameters ($rot \in [-30^\circ, -5^\circ] \cup [5^\circ, 30^\circ]$) to ensure that the original movement direction of the entity is not changed.

Translation Operator. The translation operator (TR) changes the position of the object. The operator first randomly selects the entity to be translated from the multi-view cooperative perception scene s . For each participant's viewpoint, it deletes the entity with the original position (x, y, z) and inserts the entity with the new position $(x + t_x, y + t_y, z')$. t_x and t_y are the translation distances of the object along the x and y axes, respectively. To ensure that an entity is positioned on the ground, the z' coordinate of the translated object is automatically calculated based on its coordinates on the x and y axes following the translation. Since the translation operator utilizes an insertion operation, it guarantees that the entity's translated position resides on the road.

3.3 Fitness-Guided V2X Scene Testing

In theory, the number of tests each operator can generate is endless. Therefore, we must impose limitations and guidance to ensure test quality and improve testing efficiency. To enhance the testing efficiency of V2XGEN, we propose a fitness-guided testing process for V2X cooperative perception systems under the interactive cooperation of n vehicles. The core idea of this guidance strategy is to generate scenes with occlusion relationships and long-range objects in the perspective of the ego vehicle while maximally confusing cooperative perception systems. Next, we introduce the fitness-guided strategy in detail.

Fitness Metric. We design a fitness metric that measures the likelihood of test data to reveal errors. Our fitness metric comprises two error-revealing ability scores: F_{OP} , designed to detect occlusion perception errors, and F_{LP} , intended to identify long-range perception errors.

Given a ground-truth bounding box $B_{gt} \in \mathbb{GT}$ and a predicted bounding box $B_p \in \mathbb{DT}$, the occlusion perception error score can be expressed as follows:

$$F_{OP} = \sum_{B_{gt} \in \mathbb{GT}} I_{GT}(B_{gt}, B_p) * Occ_{ego}(o_{gt}) * \prod_{i=1}^n (1 - Occ_{cv_i}(o_{gt})) \quad (4)$$

, where $I_{GT}(\cdot)$ is an indicator function equal to 1 if and only if the cooperative perception system fails to detect the object B_{gt} . $Occ_{ego}(o_{gt})$ and $Occ_{cv_i}(o_{gt})$ represent the maximum line of sight occlusion rate for the ego vehicle and the i -th cooperative vehicle, respectively, when detecting the object o_{gt} with the ground truth bounding box B_{gt} . The rationale behind the score is the cooperative perception

system should assist the ego vehicle in detecting objects with high occlusion rates, and erroneous detections by the cooperative perception system could result in severe driving accidents.

The long-range perception error score is expressed as:

$$F_{LP} = \sum_{B_{gt} \in \mathbb{GT}} I_{GT}(B_{gt}, B_p) * \frac{\min(Dis^{ego}(B_{gt}), Dis_{max}^{ego})}{Dis_{max}^{ego}} * \prod_{i=1}^n (1 - \frac{\min(Dis^{cv_i}(B_{gt}), Dis_{max}^{cv_i})}{Dis_{max}^{cv_i}}) \quad (5)$$

, where $dis^{ego}(\cdot)$ calculates the distance between a bounding box B_{gt} and the ego vehicle's LiDAR position, $dis^{cv_i}(\cdot)$ calculates the distance between a bounding box B_{gt} and the i -th cooperative vehicle's LiDAR position, dis_{max}^{ego} and $dis_{max}^{cv_i}$ are the maximum recognition distances of the LiDAR equipped by the ego vehicle and the i -th cooperative vehicle respectively. The intuition behind the score is that the cooperative perception system should aid the ego vehicle in detecting distant objects. We aim to investigate scenes in which a nearby cooperative vehicle offers limited assistance to the ego vehicle, potentially resulting in false detections.

Finally, our fitness metric can be expressed as a weighted sum of the two scores:

$$Fitness(m) = \alpha * F_{OP} + \beta * F_{LP} \quad (6)$$

, where $\alpha + \beta = 1$. Similar to the traditional software testing approach that aims to increase code coverage, V2XGEN attempts to generate a test set designed to maximize the fitness score.

Algorithm 1 Fitness-guided V2X Scene Generation

Input : The tested system CP , the transformation operator set \mathbb{A} , the set of seed scene \mathbb{S}_{ori} , the number of generated tests gen_{num} , the maximum number of entity manipulations N

Output : Generated high-quality test data \mathbb{TD}

```

1:  $\mathbb{TD} \leftarrow \emptyset$ 
2: for  $s$  in  $\mathbb{S}_{ori}$  do
3:    $\mathbb{GT} \leftarrow LoadLabel(s)$ 
4:    $s', \mathbb{GT}' \leftarrow s, \mathbb{GT}$ 
5:   for  $i=1, 2, \dots, N$  do
6:      $a = RandSelOperator(\mathbb{A})$ 
7:      $s', \mathbb{GT}' = Transform(s', \mathbb{GT}', a)$ 
8:   end for
9:    $\mathbb{DT}' = GetPred(CP, s')$ 
10:   $Occ, Dis = CalOccandDis(\mathbb{GT}', s')$ 
11:   $Fitness_{pri} = CalFitnessPri(\mathbb{DT}', \mathbb{GT}', Occ, Dis)$ 
12:   $Spc = CreateTransScene(s', \mathbb{GT}', Fitness_{pri})$ 
13:  if  $len(\mathbb{TD}) < gen_{num}$  then
14:     $\mathbb{TD}.update(Spc)$ 
15:  else
16:    if  $Spc.Fitness_{pri} > \mathbb{TD}[-1].Fitness_{pri}$  then
17:       $\mathbb{TD}[-1] = Spc$ 
18:       $\mathbb{TD}.SortByFitness()$ 
19:    end if
20:  end if
21: end for
22: return  $\mathbb{TD}$ 

```

Testing Workflow. This fitness-guided strategy enables V2XGEN to uncover more system defects with the same testing set size, thereby improving testing efficiency. Algorithm 1 presents the process of fitness-guided V2X scene generation in detail. The algorithm takes the tested system

CP , a set of scene transformation operators \mathbb{A} with the corresponding parameters, a seed set S_{ori} , the number of generated tests gen_{num} , and the maximum number of object mutation N as input. The algorithm first loads the label of the scene data s to be transformed (line 3). Then it randomly selects a transformation operator from the operator set (line 6). The virtual LiDAR sensor renders the point cloud, then synthesizes s' with the background data and generates the label GT' of the data s' (line 7). The core implementation process of this algorithm includes first putting the seed s' into the cooperative perception system for prediction. Subsequently, it calculates the distance and occlusion relationship of objects (lines 9-10), followed by the computation of the fitness guidance metric value based on the aforementioned relationship and bounding box prediction (Lines 11-12). Then, the generated test cases will be added to $\mathbb{T}\mathbb{D}$ (Lines 13-14). When the generated quantity surpasses gen_{num} (Lines 15-20), V2XGEN retains tests that are more likely to detect occlusion perception errors and long-range perception errors.

3.4 Metamorphic Relations

Manual labeling of our generated test cases can be time-consuming and labor-intensive. To alleviate this, we leverage metamorphic relations (MRs) [31], [32] to create test oracles. MRs describe the necessary properties of a target software in terms of inputs and their expected outputs. Violations of MRs often indicate potential errors.

V2XGEN is designed for cooperative perception systems based on metamorphic testing. Specifically, we denote the cooperative perception system as CP , which detects results using the multi-view cooperative perception scene $s \in \mathbb{S}$, including point clouds collected from ego and cooperative vehicles. Given a set of entity instances \mathbb{E}_{ins} , an insertion MR can be formalized as follows:

$$MR_1 : \forall e_{ins} \in \mathbb{E}_{ins} \wedge \forall s \in \mathbb{S}, \zeta \{CP[s] \cup GT_{ins}, CP[\sigma(s, e_{ins})]\} \quad (7)$$

, where σ is the insertion operator for inserting an entity instance e_{ins} into the multi-view background scene s , GT_{ins} is the ground truth of the entity e_{ins} (i.e., the estimated bounding box in object detection task) and ζ is a criterion asserting the equality of CP results. Similar to the insertion MR, given the set of background entity instances \mathbb{E}_{del} from $s \in \mathbb{S}$, the deletion MR used to test CP can be represented as follows:

$$MR_2 : \forall e_{del} \in \mathbb{E}_{del} \wedge \forall s \in \mathbb{S}, \zeta \{CP[s] \setminus GT_{del}, CP[\tau(s, e_{del})]\} \quad (8)$$

, where τ is the deletion operator for deleting an entity instance e_{del} from the multi-view background scene s , GT_{del} is the ground truth of the entity e_{del} .

MR_1 and MR_2 are built upon the following two facts: (1) the object insertion and deletion operators should not change the correct prediction of CP ; (2) the inserted object should be detected correctly, and the deleted object should not be detected. Since the remaining composite operators are combinations of insertion and deletion operators, their MR s can be automatically derived based on MR_1 and MR_2 . However, asserting equality according to Equation 7 and Equation 8 is too strict and can lead to a large number of false positives due to a slight drift in detection results. Therefore, we follow previous work [17] to leverage soft

equality criteria ζ derived from Average Precision (AP). Given the MR, we can obtain the test oracle information without manual annotation by checking if the MR is violated.

4 EXPERIMENTAL DESIGN

V2XGEN is designed to systematically test the cooperative driving system, particularly to verify its performance on long-range and occlusion perception scenes. To this end, we empirically explore the following three research questions (RQ):

- RQ1: How effective is the V2XGEN at synthesizing realistic cooperative perception data?
- RQ2: How effectively can V2XGEN generate tests under the fitness-guided scene generation?
- RQ3: How effective is V2XGEN in enhancing cooperative perception systems through retraining?

4.1 Implementation Details

In all experiments, we set the maximum number of entity manipulations N as 3 in Algorithm 1. α, β in Equation 6 are set to 0.5 and 0.5, respectively. Given that the V2V4Real [13] dataset is collected using multiple vehicles outfitted with Velodyne VLP-32 LiDAR sensors, we adopt the Velodyne VLP-32 LiDAR configuration for the construction of our virtual simulator. The distance parameter k in Equation 2 is set to 50 (m) according to the distance division of the V2V4Real dataset. We implement V2XGEN's workflow to conduct the experiments. All experiments are performed on a Ubuntu 21.10 desktop with a GeForce RTX 4070, a 16-core processor at 3.80GHz, and 32GB RAM.

4.2 Dataset

We use the V2V4Real [13] test dataset as the initial seed for transformation. V2V4Real is a real-world dataset for Vehicle-to-Vehicle cooperative perception, comprising sensor data from cooperative vehicles across diverse scenarios. It includes 347 km of highway and 63 km of city driving logs, 20,000 LiDAR frames, 240,000 annotated 3D bounding boxes, and HD maps of all routes. The open-source repository currently provides nine test scenarios. We apply our proposed technique to the original test split of the cooperative object detection dataset to identify errors in the V2X cooperative perception system. Additionally, we use ShapeNet [33] to construct entity assets \mathbb{E} for insertion. ShapeNet is a large-scale dataset of over 220,000 annotated 3D object models. For this study, we build an entity asset from the car category in ShapeNet, which consists of 3483 entities with various styles.

4.3 V2X Cooperation Perception Systems

To comprehensively evaluate the performance of our techniques, we utilize six cooperative perception systems with diverse fusion schemes in our experiment. These systems consist of one early fusion system [13], one late fusion system [13], and four state-of-the-art intermediate fusion systems (V2VNet [25], V2X-ViT [34], AttFusion [19], F-Cooper [24]). All of these perception systems are based on

LiDAR and are designed to process multi-view point clouds as input. Due to the page limit, we refer audiences to our supplementary website [35] for details of each system under test.

4.4 Evaluation Metric and Baseline Comparison

Metric. The goal of cooperative perception is to collaboratively detect objects across multiple 3D point clouds from the ego and cooperative vehicles. To evaluate cooperative 3D object detection, we first apply the IOU metric (Section 2.2) to determine successful detections. We then assess performance using Average Precision (AP), a standard metric in V2X cooperative detection research [13], [15]. For fair comparisons, we adopt the 11 recall positions from the Pascal VOC benchmark [36], defined as follows:

$$AP|_R = \frac{1}{|R|} \sum_{r \in R} \rho_{\text{interp}}(r) \quad (9)$$

We use 11 equally spaced recall levels, denoted as $R_{11} = \{0, 0.1, 0.2, \dots, 1\}$. The interpolation function, $\rho_{\text{interp}}(r) = \max_{r', r' \geq r} \rho(r')$, is employed, where $\rho(r)$ represents the precision at recall r . A higher AP reflects better performance of cooperative perception systems.

To evaluate the realism of the cooperative perception data, we utilize FRD [37] (Frechet Range Distance) as a metric to measure the realism of synthetic data. The FRD score determines the quality of synthetic LiDAR point clouds by calculating the squared Wasserstein metric between the mean and covariance of network activations in RangeNet++ [38] for both synthetic and real data. The calculation of the FRD can be represented as follows:

$$FRD(X, Y) = \|\mu_X - \mu_Y\|^2 + \text{Tr}(\Sigma_X + \Sigma_Y - 2(\Sigma_X \Sigma_Y)^{1/2}) \quad (10)$$

, where X and Y represent the distributions of the network's activations for real and synthetic data, respectively. μ represents the means of the data activations, while Σ is the covariance matrices of the activations from data. The trace of a matrix is denoted by Tr . A lower FRD score indicates greater realism in the synthetic data.

Baseline. The V2X cooperative perception system is a complex software system involving multi-agent collaboration. However, the most advanced methods for manipulating objects in point clouds primarily focus on single-agent systems. Currently, the only available testing method for cooperative perception, CooTest [15], does not support object manipulation within the scene. In order to evaluate the realism of the transformed data generated by V2X scene transformation operators in V2XGEN (i.e. RQ1), we collect corresponding point cloud data operators from state-of-the-art single-agent test generation methods as the baseline. Specifically, we leverage TauLim [16], an object-level point cloud insertion-based test generation method, as the insertion operator. The deletion operator uses the method of directly deleting the object points in the ground-truth box. The translation, rotation, and scaling follow the methods proposed in LiRTest [17]. Considering that these single-agent methods completely fail to consider the physical characteristics under V2X cooperative driving, we leverage Equation 3 to ensure that their entity manipulation across different viewpoints is as consistent as possible in the testing generation process. Finally, we compare the realism of data

generated by V2XGEN with that produced by combining these single-agent operators (denoted as *SAGen*). To evaluate the effectiveness of detecting cooperative perception system errors and optimizing them in V2XGEN (i.e., RQ2), we use the only current cooperative perception testing method called CooTest [15] and a version of V2XGEN without a fitness-guided strategy (denoted as V2XGEN_N), which retains transformation data randomly.

5 RESULT ANALYSIS

5.1 Answer to RQ1

To assess the fidelity of the data generated by the operator in the V2XGEN framework, we conduct experiments utilizing all nine cooperative driving test scenarios (i.e., driving record for a period of time) from the V2V4Real test set. Specifically, we randomly select 50 scenes as the initial seed data for each scenario and perform 1, 2, and 3 transformations on each scene in the seed data, respectively, to form three synthetic data sets (denoted as M_1 , M_2 , and M_3). For each transformation, we randomly select an operator from the set $\mathbb{A} = \{IS, DL, TR, SC, RO\}$. Throughout the data generation process, we ensure the consistency of the operators and coordinate transformations applied by both the ego vehicle and the cooperative vehicle. We then compute the FRD values of the V2XGEN and the baseline data generation method. The experiment is repeated five times, with results averaged to minimize randomness.

We further conduct a user study to evaluate the naturalness of cooperative driving data generated by each operator in V2XGEN. We recruited 22 participants from the computer science departments of four research universities, with 95.5% holding at least a master's degree in SE or CS. Among them, 14 had over one year of experience in autonomous driving or V2X, and 17 had similar experience in object detection. During the study, we randomly selected five cooperative perception data instances per transformation operator as test seeds. We then asked the participant to rank the cooperative perception data synthesized by two different generation methods from each seed through a questionnaire. Participants ranked the quality of synthesized point cloud data from two different generation methods for each seed, focusing on the realism of the ego and cooperative vehicle data frames. To mitigate bias, we randomly assigned the order of data synthesized by different generation methods for each test seed. We further refer readers to our supplementary website [35] for the complete questionnaire. After the study, we used the one-sided Wilcoxon rank-sum test [39] to assess whether any pipeline is significantly preferred by participants.

Results. Table 1 shows the realism of quantitative results in diverse cooperative perception scenarios of different data synthesis pipelines. Compared with the baseline, V2XGEN achieves the lowest FRD in all configurations. On average, the V2XGEN method reduces FRD by 5.2%, 8.6%, and 12.5% when compared to the *SAGen* method in the M_1 , M_2 , and M_3 transformation configurations, respectively. These results indicate that V2XGEN can generate high-quality and realistic cooperative perception data after the object transformation. Figure 6 depicts the participants' preferences regarding two data synthesis strategies for each

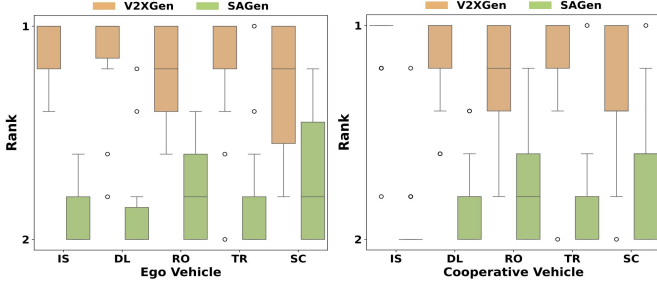


Fig. 6. Participants' choices over different data synthesis methods in cooperative data naturalness.

TABLE 1

Realism of transformed data generated across different approaches in diverse cooperative perception scenarios.

Scenario	V2XGEN			SAGen		
	M1	M2	M3	M1	M2	M3
S1	203.8	211.6	214.3	215.0	239.2	264.0
S2	190.3	197.1	193.2	193.5	210.4	225.7
S3	248.8	259.4	259.1	258.2	270.4	285.2
S4	151.4	153.2	177.8	164.5	173.1	207.1
S5	175.1	217.6	243.6	193.9	244.6	282.8
S6	143.0	157.4	169.7	146.7	168.6	197.1
S7	129.4	149.9	167.8	137.6	160.0	185.6
S8	203.6	205.4	218.4	211.0	229.2	247.1
S9	212.5	275.3	317.8	228.6	303.3	347.3
Average	184.2	203.0	218.0	194.3	222.1	249.1

transformation operator in terms of the naturalness of the point cloud. The left and right sub-figures represent the synthesized data frames of the ego vehicle and cooperative vehicle, respectively, reflecting the realism achieved after applying the transformation operator. We find that more participants prefer V2XGEN over the baseline method on all five transformation operators. Wilcoxon's rank-sum test results suggest that the mean ranking differences between V2XGEN and the second-chosen method are statistically significant ($p < 0.0001$).

Discussion. The results indicate that our V2X researchers in the field of autonomous driving generally agree that V2XGEN yields synthetic data that is realistic. These synthetic data adhere to the principles of the physical world and align with the characteristics of V2X systems. This conclusion supports the notion that the high-fidelity data generation method serves as a reasonable and effective approach for synthesizing complex V2X cooperative driving environments. Additionally, we observed that as the number of mutations increases, the divergence between the FRD of the SAGen and V2XGEN methods becomes more pronounced. Consequently, employing the single-agent method directly cannot produce realistic data for the V2X cooperative perception system. The method proposed in this paper can leverage existing V2X scenes to flexibly construct a diverse range of V2X cooperative driving scenes.

5.2 Answer to RQ2

To evaluate the effectiveness of the proposed fitness-guided V2X scene generation strategy in detecting erroneous behaviors of V2X cooperative perception systems, we randomly

TABLE 2

Testing results of cooperative perception systems on the transformed testing sets generated with different guidance approaches.

System	V2XGEN			CooTest			V2XGEN_N		
	AP	OE	LE	AP	OE	LE	AP	OE	LE
Early Fusion	53.0	2067	639	56.8	1676	346	59.3	719	372
Late Fusion	45.2	1632	609	52.1	1126	246	54.9	383	240
V2VNet	52.6	1733	973	56.8	1565	464	62.8	560	333
V2X-ViT	52.6	1891	1021	56.1	1681	483	63.1	556	417
AttFusion	53.6	1773	805	57.8	1416	356	64.0	461	376
F-Cooper	48.6	2175	1334	53.9	2102	473	59.7	625	544

TABLE 3

The occlusion and long-range perception error rates of cooperative perception test data generated through various guidance methods.

System	V2XGEN		CooTest		V2XGEN_N	
	OER	LER	OER	LER	OER	LER
Early Fusion	0.39	0.28	0.30	0.15	0.28	0.19
Late Fusion	0.31	0.28	0.20	0.14	0.17	0.13
V2VNet	0.36	0.28	0.27	0.22	0.22	0.16
V2X-ViT	0.37	0.31	0.29	0.25	0.23	0.20
AttFusion	0.35	0.25	0.25	0.18	0.20	0.18
F-Cooper	0.45	0.38	0.35	0.27	0.27	0.27

divide the original test set into two halves (T_{h1} and T_{h2}) and leverage one half (T_{h1}) as the initial seeds. To reduce randomness and cultivate diverse synthetic data, we set N to 1, 2, and 3 in Algorithm 1 to generate three distinct transformed datasets. We then combined these datasets to create a larger transformed test set. In the experiments, we apply V2XGEN, CooTest, and V2XGEN_N (w/o fitness-guided strategy) to select a specific small batch size from the generated data, enabling a comparison of the effectiveness of different guided methods in test generation. Specifically, for each guided strategy, we retain 10% and 15% of the transformed data to evaluate the effectiveness of the guidance strategies. Then we calculate the AP in generated test cases of cooperative perception systems under test for each configuration. Furthermore, we count the number of long-range and occlusion perception errors (see Section 3.1), the occlusion perception error rate (OER), and the long-distance perception error rate (LER), and visualize some typical instances of long-range perception errors and occlusion perception errors detected by V2XGEN to provide a direct understanding. The experiment is repeated three times and averaged to minimize the effect of randomness.

Results. Table 2 presents the testing results of different systems on the tests generated by three guidance approaches when retaining 15% of the transformation data. Obviously, compared to the V2XGEN_N and CooTest guidance strategy, the proposed fitness-guided V2X scene generation method can find more occlusion and long-range perception errors in all configurations. Compared to the best baseline performance, the fitness-guided V2X scene generation strategy exhibits an average effectiveness improvement of 8.4%. Furthermore, experimental results show that a large number of occlusion and long-range perception errors could lead to a sharp decline in AP. These results underscore that V2XGEN can achieve higher testing effi-

TABLE 4
The test result comparison after retraining the system with the transformed data generated by V2XGEN.

System	Transformed Dataset						Original Dataset					
	AP		OE		LE		AP		OE		LE	
	Before	After	Before	After	Before	After	Before	After	Before	After	Before	After
Early Fusion	59.1	61.0	4426	2090	2638	1469	59.6	61.9	3252	1501	1774	1004
Late Fusion	54.7	63.2	2646	1743	1563	1401	55.1	63.9	1859	1171	1118	1006
V2VNet	63.4	66.2	3399	1285	2504	2139	64.6	67.8	2427	781	1674	1468
V2X-ViT	64.1	66.4	3526	1369	2812	2016	64.9	67.1	2536	913	1907	1420
AttFusion	63.5	67.0	3210	1237	2678	1809	64.7	68.5	2229	744	1819	1253
F-Cooper	60.2	62.3	4235	1805	4110	1997	60.8	63.4	3100	1201	2826	1383

ciency by using the fitness-guided V2X scene generation method. Table 3 presents the results of testing the system’s occlusion and long-range perception error rates using data generated by various guidance methods when retaining 15% of the transformation data. Results show that V2XGen-guided data produces data with higher occlusion error rates and higher long-range perception error rates compared to other baselines. Moreover, we provide detailed results for the 10% retaining data configuration, repeated experimental results, and several visualizations of occlusion and long-range errors on the supplementary website [35].

Discussion. We examine the number and AP values of occlusion and long-range perception errors identified by the fitness-guided scene generation method. The results indicate that these errors adversely affect the performance of cooperative perception systems. Furthermore, our definitions of occlusion and long-range perception errors are rooted in the fundamental principles of V2X cooperative perception systems, which posits that such systems should assist the ego vehicle in detecting occlusions and distant objects. However, existing systems can only partially mitigate the challenges posed by individual agents. Finally, as shown in Table 3, the occlusion perception error rate for nearly all configurations is higher than that of long-range perception errors, suggesting that greater attention should be devoted to processing occlusion scenes in the software development of V2X cooperative perception systems.

5.3 Answer to RQ3

Here we investigate whether retraining the cooperative perception systems with test scenes generated by V2XGEN helps enhance the system’s performance. We apply the generated test suite in RQ2 for system retraining. To demonstrate the improvement of performance clearly, we leverage the remaining data T_{h2} (introduced in RQ2) to construct the validation set. Specifically, we utilize T_{h2} as the initial seed and set N to 1, 2, and 3 to execute Algorithm 1 for generating three distinct transformed datasets. Subsequently, we combine all these transformed datasets to create a large-scale validation set. We keep the experimental configuration of retraining consistent with the initial training system process, and the retraining epoch is set as 10. To further ensure that the retrained systems perform effectively in head scenes, we test all retrained systems on the original test scenes. The experiment is repeated three times and averaged to minimize the effect of randomness.

Results. Table 4 presents the AP, occlusion perception error numbers, and long-range perception error numbers under different perceiving ranges of all systems after retraining with the transformed data generated by V2XGEN. As shown in Table 4, it is evident regardless of the fusion scheme employed by the cooperative perception system, V2XGEN can consistently enhance the AP on the original test set and the transformed test set and mitigate occlusion perception error and long-range perception error after retraining. In comparison to the perception performance under the transformed test set before retraining, the overall improvement in AP ranges from 3.3% to 15.5%. Additionally, the average reductions in occlusion and long-range perception errors are 54.9% and 30.2%, respectively. Furthermore, the average precision of all retrained systems evaluated on the original test scenes increases by 6.4%. We report the system’s performance after each retraining on the supplementary website [35].

Discussion. Our experiments show that V2XGEN is possible to reduce occlusion perception errors and long-range perception errors by leveraging retraining techniques to increase the cooperative perception system’s overall performance. By using V2XGEN to generate realistic transformation scenes based on the collected real scenes, the system performance can be continuously optimized iteratively. However, we find that the retrained system still suffers from a variable number of occlusion and long-range perception errors. A potential explanation for this issue is the presence of a positioning error in the vehicle data from the V2V4Real dataset, as confirmed by its developer. This error may adversely affect the retraining process using data generated by V2XGEN. Given the complex structure and specific communication mechanisms inherent in V2X cooperative perception systems, it is essential to integrate specific repair technologies to enhance the system’s performance.

5.4 Threats to Validity

Data Selection. Data selection is a primary factor impacting validity. The limitation of the experimental dataset poses a risk to the generalizability of the findings. The quality of the transformed data relies heavily on the characteristics of the original dataset. As a result, if the input data includes driving scenes not present in the training set, the retrained system may encounter difficulties in making accurate predictions. To address this concern, V2XGEN employs

a variety of transformation operators and utilizes a widely used large-scale dataset for experiments, demonstrating the potential for generalization to other datasets.

Data Simulation. Data simulation introduces a potential threat to validity. Firstly, the parameter configuration of the virtual sensors and the quality of the 3D models in V2XGEN can significantly impact the quality of the synthesized data. To mitigate this, we utilize real-world LiDAR configurations in V2X systems for our virtual sensor setup and select ShapeNet, a popular source for 3D entity assets. Secondly, variability in configurable transformation parameters poses an additional potential threat. Some of our findings may not apply to different parameter sets during evaluation. To mitigate this concern, we thoughtfully select rotation and scale parameters in our experimental design to closely replicate the actual cooperative driving environment.

The Testing Functionality Selection. V2XGEN exclusively conducts offline testing [40] to identify performance issues related to occlusion and long-range detection in LiDAR-based cooperative object detection systems. Although offline testing is often indispensable for the development lifecycle of cooperative perception modules [41], the present study does not assess the influence of cooperative perception module issues on subsequent tasks such as decision-making, planning, and control.

6 RELATED WORK

Quality Assurance of ADS Perception Systems. Perception systems are crucial for supporting ADS in industrial applications, significantly affecting overall system quality [2]. Research has focused on testing the robustness of single-agent perception systems across various driving tasks [17], [18], [42]–[44]. To evaluate camera-based perception systems, a representative study [42] generates data by incorporating object instances into background images. Several studies also test LiDAR-based perception systems. LiRTesT [17] uses metamorphic relations to create test point clouds, identifying failures in 3D object detection models. Christian et al. [18] propose testing LiDAR systems by introducing semantic mutations to real-world data for the semantic segmentation task. Gao et al. present an object-insertion framework for multi-sensor fusion perception systems [45]. However, extending these single-agent testing methods to cooperative perception systems becomes challenging due to the consistent nature of the multiple perspectives required for cooperative systems. Recently, Guo et al. first proposed CooTest [15], a tool specifically designed to evaluate cooperative perception systems under extreme conditions (e.g., communication interference, adverse weather, etc.). Although CooTest provides valuable insights into system robustness, it lacks consideration of traffic participants and does not support flexible modifications to their number, styles, or spatial relationships within a scene. This limitation significantly reduces the diversity of the generated scenes. In contrast, V2XGEN addresses this gap by leveraging a series of operators to manipulate entities rigorously within scenes, enabling the flexible generation of realistic, diverse, and challenging traffic scenes that better reflect real-world conditions.

Metamorphic Testing. Metamorphic Testing (MT) [31], [46] is a software testing methodology that alleviates the test oracle problem by identifying software bugs through the detection of deviations from domain-specific metamorphic relations defined across outputs from multiple executions of the program with various test inputs. With the rapid progression of deep learning, metamorphic testing has been applied in both classification and regression tasks [15], [17], [42], [47]–[49]. Xie et al. [47] introduced an MT technique to test machine learning classification algorithms, demonstrating its effectiveness in identifying errors within a widely recognized open-source classification program. In addition, Wang et al. [42] employed MT as an adaptive and effective testing strategy by comparing object detection results between original and synthetic images to uncover defects in object detection systems. Guo et al. [17] introduced LiDAR-based specific metamorphic relations and utilized them to generate various corner test cases. Furthermore, CooTest [15] developed a specific V2X-oriented metamorphic testing module for cooperative perception systems.

7 CONCLUSION

In this paper, we present V2XGEN, the tool for generating test scenes tailored specifically for V2X communication systems. V2XGEN utilizes a high-fidelity approach to render object instances and ground point clouds using a set of virtual sensors. It then synthesizes realistic cooperative perception data by simulating object instances in valid yet challenging locations within the target scene. Furthermore, V2XGEN incorporates fitness metric guidance to enhance testing efficiency and effectiveness. The experimental results on six state-of-the-art cooperative detection systems across various fusion schemes illustrate that V2XGEN adeptly detects erroneous behavior in the systems under test and enhances a system’s robustness through retraining.

REFERENCES

- [1] J. Zhao, W. Zhao, B. Deng, Z. Wang, F. Zhang, W. Zheng, W. Cao, J. Nan, Y. Lian, and A. F. Burke, “Autonomous driving system: A comprehensive survey,” *Expert Syst. Appl.*, vol. 242, p. 122836, 2024. [Online]. Available: <https://doi.org/10.1016/j.eswa.2023.122836>
- [2] Y. Li and J. Ibanez-Guzman, “Lidar for autonomous driving: The principles, challenges, and trends for automotive lidar and perception systems,” *IEEE Signal Processing Magazine*, vol. 37, no. 4, pp. 50–61, 2020.
- [3] L.-H. Wen and K.-H. Jo, “Deep learning-based perception systems for autonomous driving: A comprehensive survey,” *Neurocomputing*, vol. 489, pp. 255–270, 2022.
- [4] “Tesla’s autopilot was engaged when model 3 crashed into truck, report states,” 2019. [Online]. Available: <https://www.theverge.com/2019/5/16/18627766/tesla-autopilot-fatal-crash-delray-florida-ntsb-model-3>
- [5] S. Kochanthara, T. Singh, A. Forrai, and L. Cleophas, “Safety of perception systems for automated driving: A case study on apollo,” *ACM Trans. Softw. Eng. Methodol.*, vol. 33, no. 3, pp. 64:1–64:28, 2024. [Online]. Available: <https://doi.org/10.1145/3631969>
- [6] G. Cui, W. Zhang, Y. Xiao, L. Yao, and Z. Fang, “Cooperative perception technology of autonomous driving in the internet of vehicles environment: A review,” *Sensors*, vol. 22, no. 15, p. 5535, 2022.
- [7] Y. Ma, J. Lu, C. Cui, S. Zhao, X. Cao, W. Ye, and Z. Wang, “Macp: Efficient model adaptation for cooperative perception,” in *Proceedings of the IEEE/CVF Winter Conference on Applications of Computer Vision*, 2024, pp. 3373–3382.

- [8] S. Hu, Z. Fang, Y. Deng, X. Chen, and Y. Fang, "Collaborative perception for connected and autonomous driving: Challenges, possible solutions and opportunities," *CoRR*, vol. abs/2401.01544, 2024. [Online]. Available: <https://doi.org/10.48550/arXiv.2401.01544>
- [9] "Astri and baidu apollo collaborate to promote the implementation of c-v2x technology in hong kong," <https://www.astri.org/news-detail/astri-and-baidu-apollo-collaborate-to-promote-the-implementation-of-c-v2x-technology-in-hong-kong/>, 2023.
- [10] "V2v and v2x technology paves the way for autonomous driving," <https://www.assemblymag.com/articles/98013-v2v-and-v2x-technology-paves-the-way-for-autonomous-driving>, 2023.
- [11] Y. Han, H. Zhang, H. Li, Y. Jin, C. Lang, and Y. Li, "Collaborative perception in autonomous driving: Methods, datasets, and challenges," *IEEE Intell. Transp. Syst. Mag.*, vol. 15, no. 6, pp. 131–151, 2023. [Online]. Available: <https://doi.org/10.1109/ITS.2023.3298534>
- [12] T. Huang, J. Liu, X. Zhou, D. C. Nguyen, M. R. Azghadi, Y. Xia, Q. Han, and S. Sun, "V2X cooperative perception for autonomous driving: Recent advances and challenges," *CoRR*, vol. abs/2310.03525, 2023. [Online]. Available: <https://doi.org/10.48550/arXiv.2310.03525>
- [13] R. Xu, X. Xia, J. Li, H. Li, S. Zhang, Z. Tu, Z. Meng, H. Xiang, X. Dong, R. Song *et al.*, "V2v4real: A real-world large-scale dataset for vehicle-to-vehicle cooperative perception," in *Proceedings of the IEEE/CVF Conference on Computer Vision and Pattern Recognition*, 2023, pp. 13712–13722. [Online]. Available: <https://doi.org/10.1109/CVPR52729.2023.01318>
- [14] H. Yu, Y. Luo, M. Shu, Y. Huo, Z. Yang, Y. Shi, Z. Guo, H. Li, X. Hu, J. Yuan, and Z. Nie, "DAIR-V2X: A large-scale dataset for vehicle-infrastructure cooperative 3d object detection," in *IEEE/CVF Conference on Computer Vision and Pattern Recognition, CVPR 2022, New Orleans, LA, USA, June 18-24, 2022*. IEEE, 2022, pp. 21329–21338. [Online]. Available: <https://doi.org/10.1109/CVPR52688.2022.02067>
- [15] A. Guo, X. Gao, Z. Chen, Y. Xiao, J. Liu, X. Ge, W. Sun, and C. Fang, "Cootest: An automated testing approach for V2X communication systems," in *Proceedings of the 33rd ACM SIGSOFT International Symposium on Software Testing and Analysis, ISSTA 2024, Vienna, Austria, September 16-20, 2024*, M. Christakis and M. Pradel, Eds. ACM, 2024, pp. 1453–1465. [Online]. Available: <https://doi.org/10.1145/3650212.3680373>
- [16] J. Lin, J. Liu, Q. Zhang, X. Zhang, and C. Fang, "Taulim: Test data augmentation of lidar point cloud by metamorphic relation," in *44th IEEE/ACM International Conference on Software Engineering: Companion Proceedings, ICSE Companion 2022, Pittsburgh, PA, USA, May 22-24, 2022*. ACM/IEEE, 2022, pp. 217–221. [Online]. Available: <https://doi.org/10.1145/3510454.3516860>
- [17] A. Guo, Y. Feng, and Z. Chen, "Lirtest: augmenting lidar point clouds for automated testing of autonomous driving systems," in *ISSTA '22: 31st ACM SIGSOFT International Symposium on Software Testing and Analysis, Virtual Event, South Korea, July 18 - 22, 2022*, S. Ryu and Y. Smaragdakis, Eds. ACM, 2022, pp. 480–492. [Online]. Available: <https://doi.org/10.1145/3533767.3534397>
- [18] G. Christian, T. Woodlief, and S. Elbaum, "Generating realistic and diverse tests for lidar-based perception systems," in *2023 IEEE/ACM 45th International Conference on Software Engineering (ICSE)*. IEEE, 2023, pp. 2604–2616. [Online]. Available: <https://doi.org/10.1109/ICSE48619.2023.00217>
- [19] R. Xu, H. Xiang, X. Xia, X. Han, J. Li, and J. Ma, "Opv2v: An open benchmark dataset and fusion pipeline for perception with vehicle-to-vehicle communication," in *2022 International Conference on Robotics and Automation (ICRA)*. IEEE, 2022, pp. 2583–2589.
- [20] L. Hobert, A. Festag, I. Llatser, L. Altomare, F. Visintainer, and A. Kovacs, "Enhancements of v2x communication in support of cooperative autonomous driving," *IEEE communications magazine*, vol. 53, no. 12, pp. 64–70, 2015.
- [21] C. Jung, D. Lee, S. Lee, and D. H. Shim, "V2x-communication-aided autonomous driving: System design and experimental validation," *Sensors*, vol. 20, no. 10, p. 2903, 2020.
- [22] Q. Chen, S. Tang, Q. Yang, and S. Fu, "Cooper: Cooperative perception for connected autonomous vehicles based on 3d point clouds," in *Proceedings of the 39th International Conference on Distributed Computing Systems*. Dallas, TX, USA: IEEE, July 7-10 2019, pp. 514–524.
- [23] Z. Y. Rawashdeh and Z. Wang, "Collaborative automated driving: A machine learning-based method to enhance the accuracy of shared information," in *2018 21st International Conference on Intelligent Transportation Systems (ITSC)*. IEEE, 2018, pp. 3961–3966.
- [24] Q. Chen, X. Ma, S. Tang, J. Guo, Q. Yang, and S. Fu, "F-cooper: feature based cooperative perception for autonomous vehicle edge computing system using 3d point clouds," in *Proceedings of the 4th Symposium on Edge Computing*. Arlington, Virginia, USA: ACM, November 7-9 2019, pp. 88–100.
- [25] T.-H. Wang, S. Manivasagam, M. Liang, B. Yang, W. Zeng, and R. Urtasun, "V2vnet: Vehicle-to-vehicle communication for joint perception and prediction," in *Computer Vision—ECCV 2020: 16th European Conference, Glasgow, UK, August 23–28, 2020, Proceedings, Part II 16*. Springer, 2020, pp. 605–621.
- [26] R. Padilla, S. L. Netto, and E. A. Da Silva, "A survey on performance metrics for object-detection algorithms," in *2020 international conference on systems, signals and image processing (IWSSIP)*. IEEE, 2020, pp. 237–242.
- [27] T. Cortinhal, G. Tzelepis, and E. E. Aksoy, "Salsanext: Fast, uncertainty-aware semantic segmentation of lidar point clouds," in *Advances in Visual Computing - 15th International Symposium, ISVC 2020, San Diego, CA, USA, October 5-7, 2020, Proceedings, Part II*, ser. Lecture Notes in Computer Science, G. Bebis, Z. Yin, E. Kim, J. Bender, K. Subr, B. C. Kwon, J. Zhao, D. Kalkofen, and G. Baci, Eds., vol. 12510. Springer, 2020, pp. 207–222. [Online]. Available: https://doi.org/10.1007/978-3-030-64559-5_16
- [28] Y. Wang, X. Chen, Y. You, L. E. Li, B. Hariharan, M. E. Campbell, K. Q. Weinberger, and W. Chao, "Train in germany, test in the USA: making 3d object detectors generalize," in *2020 IEEE/CVF Conference on Computer Vision and Pattern Recognition, CVPR 2020, Seattle, WA, USA, June 13-19, 2020*. Computer Vision Foundation / IEEE, 2020, pp. 11710–11720. [Online]. Available: https://openaccess.thecvf.com/content_CVPR_2020/html/Wang_Train_in_Germany_Test_in_the_USA_Making_3D_Object_CVPR_2020_paper.html
- [29] S. Li, Z. Wang, F. Juefei-Xu, Q. Guo, X. Li, and L. Ma, "Common corruption robustness of point cloud detectors: Benchmark and enhancement," *IEEE Transactions on Multimedia*, 2023.
- [30] A. Miller, K. Rim, P. Chopra, P. Kelkar, and M. Likhachev, "Cooperative perception and localization for cooperative driving," in *2020 IEEE International Conference on Robotics and Automation, ICRA 2020, Paris, France, May 31 - August 31, 2020*. IEEE, 2020, pp. 1256–1262. [Online]. Available: <https://doi.org/10.1109/ICRA40945.2020.9197463>
- [31] T. Y. Chen, F.-C. Kuo, H. Liu, P.-L. Poon, D. Towey, T. Tse, and Z. Q. Zhou, "Metamorphic testing: A review of challenges and opportunities," *ACM Computing Surveys (CSUR)*, vol. 51, no. 1, pp. 1–27, 2018.
- [32] T. Y. Chen, S. C. Cheung, and S. Yiu, "Metamorphic testing: A new approach for generating next test cases," *CoRR*, vol. abs/2002.12543, no. 1, pp. 1–11, 2020.
- [33] A. X. Chang, T. Funkhouser, L. Guibas, P. Hanrahan, Q. Huang, Z. Li, S. Savarese, M. Savva, S. Song, H. Su *et al.*, "Shapenet: An information-rich 3d model repository," *arXiv preprint arXiv:1512.03012*, 2015.
- [34] R. Xu, H. Xiang, Z. Tu, X. Xia, M.-H. Yang, and J. Ma, "V2x-vit: Vehicle-to-everything cooperative perception with vision transformer," in *European conference on computer vision*. Springer, 2022, pp. 107–124.
- [35] "Supplementary website," <https://sites.google.com/view/v2xgen/>, 2025.
- [36] M. Everingham, L. Van Gool, C. K. Williams, J. Winn, and A. Zisserman, "The pascal visual object classes (voc) challenge," *International journal of computer vision*, vol. 88, pp. 303–338, 2010. [Online]. Available: <https://doi.org/10.1007/s11263-009-0275-4>
- [37] V. Zyrianov, X. Zhu, and S. Wang, "Learning to generate realistic lidar point clouds," in *Computer Vision - ECCV 2022 - 17th European Conference, Tel Aviv, Israel, October 23-27, 2022, Proceedings, Part XXIII*, ser. Lecture Notes in Computer Science, S. Avidan, G. J. Brostow, M. Cissé, G. M. Farinella, and T. Hassner, Eds., vol. 13683. Springer, 2022, pp. 17–35. [Online]. Available: https://doi.org/10.1007/978-3-031-20050-2_2
- [38] A. Milioto, I. Vizzo, J. Behley, and C. Stachniss, "Rangenet ++: Fast and accurate lidar semantic segmentation," in *2019 IEEE/RSJ International Conference on Intelligent Robots and Systems, IROS 2019, Macau, SAR, China, November 3-*

- 8, 2019. IEEE, 2019, pp. 4213–4220. [Online]. Available: <https://doi.org/10.1109/IROS40897.2019.8967762>
- [39] J. Cuzick, “A wilcoxon-type test for trend,” *Statistics in medicine*, vol. 4, no. 1, pp. 87–90, 1985.
- [40] A. Stocco, B. Pulfer, and P. Tonella, “Model vs system level testing of autonomous driving systems: a replication and extension study,” *Empir. Softw. Eng.*, vol. 28, no. 3, p. 73, 2023. [Online]. Available: <https://doi.org/10.1007/s10664-023-10306-x>
- [41] F. U. Haq, D. Shin, S. Nejati, and L. C. Briand, “Can offline testing of deep neural networks replace their online testing?” *Empir. Softw. Eng.*, vol. 26, no. 5, p. 90, 2021. [Online]. Available: <https://doi.org/10.1007/s10664-021-09982-4>
- [42] S. Wang and Z. Su, “Metamorphic object insertion for testing object detection systems,” in *35th IEEE/ACM International Conference on Automated Software Engineering, ASE 2020, Melbourne, Australia, September 21–25, 2020*. IEEE, 2020, pp. 1053–1065. [Online]. Available: <https://doi.org/10.1145/3324884.3416584>
- [43] X. Xie, Y. Duan, S. Chen, and J. Xuan, “Towards the robustness of multiple object tracking systems,” in *2022 IEEE 33rd International Symposium on Software Reliability Engineering (ISSRE)*. IEEE, 2022, pp. 402–413. [Online]. Available: <https://doi.org/10.1109/ISSRE55969.2022.00046>
- [44] X. Gao, Z. Wang, Y. Feng, L. Ma, Z. Chen, and B. Xu, “Benchmarking robustness of ai-enabled multi-sensor fusion systems: Challenges and opportunities,” in *Proceedings of the 31st ACM Joint European Software Engineering Conference and Symposium on the Foundations of Software Engineering, 2023*, pp. 871–882. [Online]. Available: <https://doi.org/10.1145/3611643.3616278>
- [45] —, “Multitest: Physical-aware object insertion for testing multi-sensor fusion perception systems,” in *Proceedings of the 46th IEEE/ACM International Conference on Software Engineering, ICSE 2024, Lisbon, Portugal, April 14–20, 2024*. ACM, 2024, pp. 139:1–139:13. [Online]. Available: <https://doi.org/10.1145/3597503.3639191>
- [46] S. Segura, G. Fraser, A. B. Sanchez, and A. Ruiz-Cortés, “A survey on metamorphic testing,” *IEEE Transactions on software engineering*, vol. 42, no. 9, pp. 805–824, 2016. [Online]. Available: <https://doi.org/10.1109/TSE.2016.2532875>
- [47] X. Xie, J. W. K. Ho, C. Murphy, G. E. Kaiser, B. Xu, and T. Y. Chen, “Testing and validating machine learning classifiers by metamorphic testing,” *J. Syst. Softw.*, vol. 84, no. 4, pp. 544–558, 2011. [Online]. Available: <https://doi.org/10.1016/j.jss.2010.11.920>
- [48] Z. Q. Zhou and L. Sun, “Metamorphic testing of driverless cars,” *Commun. ACM*, vol. 62, no. 3, pp. 61–67, 2019. [Online]. Available: <https://doi.org/10.1145/3241979>
- [49] A. Guo, Y. Feng, Y. Cheng, and Z. Chen, “Semantic-guided fuzzing for virtual testing of autonomous driving systems,” *J. Syst. Softw.*, vol. 212, p. 112017, 2024. [Online]. Available: <https://doi.org/10.1016/j.jss.2024.112017>